

Helicase activity as a propagating front

Somendra M. Bhattacharjee*

Institute of Physics, Bhubaneswar 751 005, India

(Dated: February 21, 2019)

We develop a propagating front analysis, in terms of a local probability of zipping, for the helicase activity of opening up a double stranded DNA (dsDNA). In a fixed-distance ensemble (conjugate to the fixed-force ensemble) the front separates the zipped and unzipped phases of a dsDNA and a drive acts locally around the front. Bounds from variational analysis and numerical estimates for the speed of a helicase are obtained. Different types of helicase behaviours can be distinguished by the nature of the drive.

A helicase moves along a DNA and unwinds it. Whenever a double stranded DNA in a cell needs to be opened up, a helicase is summoned, be it during the semi-conservative replication, repair mechanism of a stalled process or other DNA related activities[1]. A large number of helicases including rna-helicases have so far been identified from different pro- and eucaryotes. A well-studied bacterium like *E. Coli* contains at least 17 different helicases, though the need and the function of each of these are not yet clear.

The helicase activity involves a motor action fed by NTP's (nucleotide triphosphate) and eventual opening of DNA by dissociating successive base pairs along the chain[2]. Quantitative estimates of rates of such activities (~ 400 base pair per second or less) for almost all helicases are known from *in-vitro* studies in solutions and more recently from single molecular experiments. Attempts to categorize these varieties of helicases as per their common features have led to various classification schemes. These are: (i) active vs passive depending on the direct requirement of NTP for the opening; (ii) families and superfamilies (SF) based on the conserved motifs of the primary sequence; (iii) monomeric, dimeric, hexameric, oligomeric depending on the number of units required for activity; and (iv) mode of translocation: whether it translocates on the single stands of DNA or on dsDNA. For example, dnaB, the main helicase involved in the replication of DNA in *E. Coli*, is

a hexameric, passive helicase belonging to the dnaB-like family translocating on a single strand DNA[3]. PcrA is an active, SF1, monomeric helicase translocating on ssDNA[4] while recG is an active, SF2, monomeric, ds-DNA translocating helicase[6]. Apart from these gross classifications, very little information is available on the detailed mechanism of the helicase activity.

Crystallographic data available for a few helicases have been used to model mechanisms for specific helicases. Though crystal structures cannot give a dynamic view, such proposals, attractive no doubt, are the only ones available so far. According to these proposals, hexameric helicase like dnaB, opens up dsDNA like a wedge by virtue of its motor action on ssDNA[3]. A rolling mechanism has been proposed for dimeric helicases[5]. In case of PcrA, the helicase activity and the motor action can be decoupled. Crystal structure, supplemented by biochemical evidences on mutants, favours a mechanism where the helicase moves forward on ss-DNA and during its sojourn a different domain of the helicase pulls a few bases of a strand of the ds-DNA beyond the Y-fork, the junction between ss and ds-DNA[4]. See Fig. 1 for a schematic diagram. RecG is more complicated because it moves in opposite direction from zipped to unzipped, a fork reversal process forming a Holliday junction of 4 dna strands[6].

Our aim is to develop a generic physical picture that could be applicable to all the different types of helicases. Recently, a phase coexistence based mechanism for helicase activity has been proposed by Bhattacharjee and Seno[7]. A kinetic model has also been proposed recently[8] and a random walk model was used in an earlier study[9] to analyze the movement on DNA. The phase-coexistence mechanism is based on the unzipping phase transition of a ds-DNA by a force, which was first shown in a continuum model in Ref. [10]. This transition has since then been established by exact calculations for lattice models in all dimensions[11, 12], in studies of dynamics[11, 13], by scaling theories[14], in quenched averaged DNA[15], and others. The key points of the mechanism[7] are the following. (a) A helicase keeps two single strands of a dsDNA at a separation much bigger than the base-pair separation of a ds-DNA. (b) The resulting fixed-distance ensemble for a dsDNA breaks it up

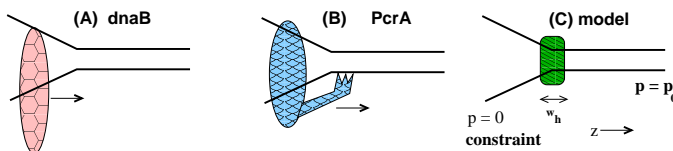


FIG. 1: Schematic representation of the two types of mechanism advocated so far (A) for dnaB type hexameric helicase, and (B) for PcrA type active monomeric helicase. The arrow indicates the overall direction of motion. (C) Proposed model. Constraints are that the DNA is open on one side while it is zipped at the other end, both phases coexisting. The shaded box of width w_h encompassing the Y-fork or interfacial or domain-wall is the region within which the unzipped phase is preferred.

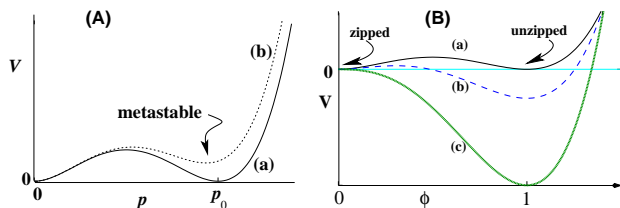


FIG. 2: Plot of $V(p)$ of Eq. (1). The solid curve in (A) shows the co-existence of the two phases, the zipped ($p = p_0$) and the unzipped one ($p = 0$). The dotted curve shows the local change near the interface or domain wall due to the drive that makes the zipped phase locally metastable or unstable. The rescaled form of the free energy (see Eq. (5)) is shown in (B). Here the zipped phase is at $\phi = 0$ which is rendered metastable (b) or unstable (c) with respect to the unzipped phase ($\phi = 1$) by changing h in Eq. (5). The relaxation due to the elastic term leads to a traveling front solution.

into a zipped phase and an unzipped phase separated by a domain wall. (c) The domain wall is identified as the Y-fork junction. All helicases act at or near this junction of the ds-ss DNA. (d) the motor action of the helicase leads to a shift in the position of the fixed-distance constraint thereby shifting the domain wall towards the zipped phase. Additional features are needed for efficiency, job-requirement and processivity (the distribution of the length unzipped before a helicase drops off). Our purpose in this paper is to use this coexistence hypothesis to develop a simple coarse grained model of the propagation of the Y-fork.

We use the zipping probability $p(z)$, the probability that the base pair at index or contour length z (measured along the backbone) is zipped as the basic variable. The unzipping transition by a force has hitherto been studied by using polymer models. However, in the case of the conjugate fixed distance ensemble, the probability of zipping, $p(z)$, under the imposed constraints, has been shown to be a useful description[7, 16]. Since the unzipping transition is of first order nature with a co-existence on the phase boundary, the state of the DNA can be described by a Landau-type hamiltonian or free energy. In addition, the presence of the helicase can be represented by the boundary conditions on two sides of the DNA (zipped on one side and unzipped on the other). The effect of the motor action that pushes (or pulls) one phase into the other and any other destabilizing effects of the helicase are taken into account by additional terms involving the zipping probability $p(z)$. We show the existence of a traveling front solution (i.e. a propagating front of Y-fork) and then get the speed of the front in terms of the parameters of the hamiltonian. A variational principle is used to derive bounds on the selected velocity.

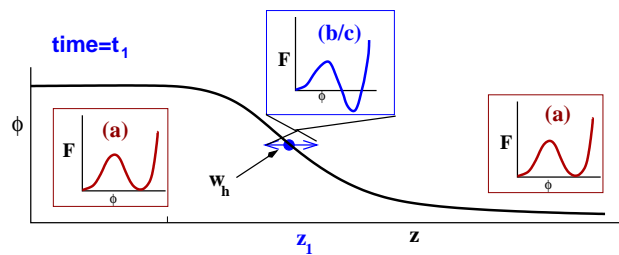


FIG. 3: Schematic representation of the pulse at an arbitrary time t_1 when the front is at location z_1 (filled circle at $\phi = 0.5$). The effective free energy is of form (b) or (c) of Fig. 2 (metastable or unstable) only within $z_1 \pm w_h$. The drive or pulse moves with the front.

The unzipping transition can be described by a Landau-type hamiltonian or free energy

$$H_0 = \int dz \left[\frac{K}{2} \left(\frac{\partial p(z)}{\partial z} \right)^2 + V(p(z)) \right],$$

$$\text{with } V(p) = \frac{1}{2} r p^2 + \frac{1}{3} w p^3 + \frac{1}{4} u p^4, \quad (1)$$

where K is the appropriate rigidity modulus, and the cubic term ensures a first order transition. The details of the phase boundary etc are in the coefficients r, w and u . Our interest is mostly in the region with $w < 0, u > 0$. Using Eq. (1) as the meanfield free energy[17] the dynamics of unzipping is given by the overdamped equation of motion

$$\Gamma^{-1} \frac{\partial p(z)}{\partial t} = - \frac{\delta H_0}{\delta p(z)} \quad (2)$$

with appropriate transport coefficient Γ . Since we are away from critical points and interested in nonequilibrium propagation problem, we may ignore noise terms in the equation of motion. Stochastic terms would also be required to describe processivity, which we do not consider in this paper.

For a long chain, with the boundary conditions $p(z) \rightarrow p_0$ (probability in the zipped phase) as $z \rightarrow +\infty$ and $p(z) \rightarrow 0$ as $z \rightarrow -\infty$ at phase coexistence, the variation of the equilibrium probability of zipping is described by the equation

$$K \frac{d^2 p(z)}{dz^2} = V'(p) \quad (3)$$

with prime denoting derivative with respect to the argument. For the assigned boundary condition, there is a domain wall solution located at an arbitrarily chosen $z = 0$ with a profile $\int_0^p dp / \sqrt{2V(p)/K} = z$, and $p(z)$ decays exponentially in the zipped phase as $p(z) \sim \exp(-V''(p_0) |z| / \sqrt{K})$. The width W of the domain wall can be estimated by minimizing the energy of the wall $E = K \frac{p_0^2}{W} + \Delta E W$, where ΔE is the height of the

energy barrier separating the two minima of the potential in Eq. (1). We get $W = (Kp_0^2/\Delta E)^{1/2}$. This is an equilibrium situation that can be obtained by keeping the helicase static on dsDNA, e.g. by denying ATP in *in vitro* experiments. Since such configurations can now be prepared[18], detailed characterisation of the wall can be done experimentally.

In order to incorporate the effect of the motion of the helicase, we introduce a moving perturbation that tends to destabilize the domain wall at its current location. A time dependent perturbation is introduced in the equation of motion Eq. (2), or, equivalently, in the Hamiltonian of Eq. (1), that favours the unzipped state over a region of width w_h around the domain wall, maintaining co-existence elsewhere. See Figs. 2 and 3. The equation of motion, augmented by a “drive” term, is now given by

$$\Gamma \frac{\partial p(z)}{\partial t} = K \frac{\partial^2 p}{\partial z^2} - rp + wp^2 - up^3 - h(z,t)V_1(p),$$

with $h(z,t) = \mathcal{U}\left(\frac{z-ct}{w_h}\right).$ (4)

This is equivalent to adding a term $\int dz h(z,t)V_1(p)$ in the Hamiltonian, Eq. (1), such that the drive favours the unzipped region ($p = 0$) in a region of width w_h around $z = ct$, with the front position at $t = 0$ chosen as origin $z = 0$. In Eq. (4), $V_1(p)$ should have the right form for $V(p) + V_1(p)$ to favour the unzipped phase. A simple choice would be $V_1(p) = p^4$, though a more symmetrical form is useful. Since the helicase works only near the interface or the front, $\mathcal{U}(x)$ is a short range function. Here again for simplicity, we choose $\mathcal{U}(x) = \Delta u$ for $|x| \leq 1$ and zero otherwise. The “drive” is attached to the front and moves to the zipped side with a speed c which is to be determined self-consistently so that the front also moves with the same speed.

The role of the drive term is to disturb the coexistence between $p = 0$ (unzipped) and $p = p_0$ (zipped phase). By a transformation of variables, like $p = p_0 - \phi$ and rescaling, we recast Eq. (4) in a more standard and symmetrical form

$$\frac{\partial \phi(z)}{\partial t} = \frac{\partial^2 \phi}{\partial z^2} + f(\phi), \quad \text{where} \quad (5)$$

$$f(\phi) = \left(-\frac{1}{3} + h(z,t)\right)\phi + \phi^2 - \left(\frac{2}{3} + h(z,t)\right)\phi^3,$$

where, for brevity, same notation h is used for the drive. Another choice could have been $f(\phi) = \phi(1-\phi)(\phi - \frac{1}{2} - h(z,t))$ which is identical to Eq. (5) upto a scale transformation if and only if $h = \text{constant}$. In any case no fundamental difference is expected among the various choices mentioned. With the above form Eq. (5), there is a coexistence of the zipped phase ($\phi = 0$) and the unzipped phase ($\phi = 1$) if $h = 0$. With $h \neq 0$, the two phases are still at $\phi = 0$, and 1, with $\phi = 0$ as metastable for $0 < h < 1/3$ and unstable for $h > 1/3$. See Fig. 2.

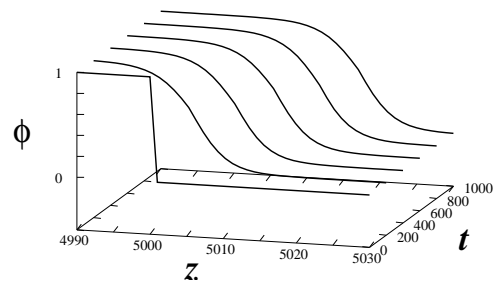


FIG. 4: Positions of the front or domain-wall for $\Delta u = 0.2$ at bulk coexistence are shown by plotting $p(z)$ vs z . The curves are at times 0, 200, 400, 600, 800, 1000 in arbitrarily chosen time units obtained from a discretized version of Eq. (5).

The symmetrical form helps in identifying the location of the front by $\phi = 0.5$ and the drive $h(z,t)$ is operative only around that point.

Assuming that the front propagates with a velocity c , i.e. $\phi(z,t) = \phi(z-ct)$, We can use the comoving frame with coordinate $\xi = z - ct$ to rewrite Eq. (4) as

$$\frac{\partial^2 \phi}{\partial \xi^2} + c \frac{\partial \phi(z)}{\partial \xi} + \frac{\partial}{\partial \phi} [V(\phi) + V_1(\phi)] = 0, \quad (6)$$

which has a mechanical analogy of a particle moving in a potential $-V(\phi)$ under friction (taking ξ as a time like variable). This analogy immediately tells us (using first integral or energy conservation) that to satisfy the boundary conditions at $\xi = \pm\infty$ when $h = 0$, one must have $c = 0$. In other words, there is no propagating solution as we might expect in the case of phase coexistence.

A propagating solution is expected if the drive h is not zero. The speed of propagation c is expected to be insensitive to width w_h of the pulse if $w_h \gg$ the width of the front or interface. In that large w_h limit, the speed should be that of a propagating front for a uniformly metastable ($h < 1/3$) or unstable ($h \geq 1/3$) case. In the uniform situation $h(z,t) = \text{constant}$, there is a pushed to pulled transition[17] in the propagation of the front at $h = 4/3$. Beyond $h = 4/3$ the velocity is determined by the linearized equation of motion while the full non-linearity is important for $h < 4/3$. For the metastable case ($h < 1/3$) any initial condition $\phi_0(z) = \phi(z, t = 0)$ will rapidly evolve to a steady shape with a velocity $c^\dagger(h) = 3h/\sqrt{2((2/3) + h)}$. The approach to this steady speed is exponentially fast in time. For the unstable case, a sharp interface (say a sharp step at $t = 0$) also evolves to this “pushed” front so long $h \leq 4/3$. However a flatter interface would maintain its flatness and move with a speed determined by the initial flatness. In the pulled limit, ($h > 4/3$), the asymptotic speed is the linearized speed $c^*(h) = 2\sqrt{h - (1/3)}$ which is reached algebraically in time provided the initial condition is sharp (e.g. a step function).

With a pulse, one may use the particle mechanics analogy that a particle is in one of the peaks of the equal

height double peaked potential $-V(\phi)$ at $\xi = -\infty$ and then at finite time it gets a push (energy input in particle mechanics) which should be sufficient to overcome frictional loss and reach the other peak at $\xi = +\infty$. This will satisfy the boundary conditions at $\xi = \pm\infty$. A moving front is therefore possible. In other words the moving front originates from the “elastic term” that tries to spread out the change in ϕ in the front region.

For a quantitative analysis of the speed, we use the variational principle developed by Benguria and Depassier[19]. If the equation of motion admits, as we verify numerically below, a monotonic front $\phi(z, t) = q(\xi)$, then the inverse mapping can be used to get ξ from q with $0 \leq q \leq 1$. Then for any positive function $g(q)$ with $-dg/dq > 0$,

$$c^2 \geq 2 \frac{\int_0^1 f g dq}{\int_0^1 -(g^2/g') dq}, \quad (7)$$

provided the integrals exist. This requires $f'(0) < 0$ for bistable f of the form Eq. (5). We consider only this metastable case for this analysis here, though the other situation with $f'(0) > 0$ (unstable case) can also be treated in a slightly different way. Taking $g(q) = [(1-q)/q]^b$ and the uniform case of f i.e. $h(z, t) = h$, one gets

$$c^2 \geq \frac{-b^2}{6} + \frac{1}{4} h b (6 - b). \quad (8)$$

The supremum of the lower bound at $b = 3h/[2((2/3) + h)]$ recovers the exact velocity, c^\dagger , mentioned earlier (valid for $h < 1/3$). Under the assumption of monotonicity, the pulse, in q -space, is at $q = 1/2$ and is of width $\Omega(w_h)$ such that $\Omega(w_h \rightarrow \infty) = 1/2$. The profile $q(\xi)$ generally approaches the two limits exponentially as we have seen in Eq. (3) and therefore $\tilde{\Omega} \equiv (1/2) - \Omega \sim \exp(-w_h/w^*)$ with some characteristic length w^* . The pulse term contribution to the numerator of the bound of Eq. (7) is an integral of $q(1 - q^2)g(q)$ over $q \in [\tilde{\Omega}, 1 - \tilde{\Omega}]$ and the integral can be expressed in terms of incomplete beta functions. We then obtain

$$c^2 \geq \frac{-b^2}{6} + \frac{1}{4} \Delta u b (6 - b) - A(\tilde{\Omega}, b) \Delta u b, \quad (9)$$

where the form of $A(\tilde{\Omega}, b) (\geq 0)$ is not displayed. Taking the maximum of the right hand side as the best estimate $c(w_h)$ for the speed, we see that $c(w_h) < c^\dagger$ (the bulk value), as expected. Using the asymptotic behaviour of the incomplete beta functions in $A(\tilde{\Omega}, b)$, one finds that $c(w)$ saturates exponentially for large w_h . In the other limit of small w_h (equivalent to small Ω), there is a linear dependence on w_h . Combining these, we may write $c(w) = c_0[1 - a \exp(-w/w_0)]$, a form that does represent the numerical data very well.

In order to determine the velocity of propagation of the front with a pulse, we have numerically solved a discretized version of Eq. (6) for various values of the width

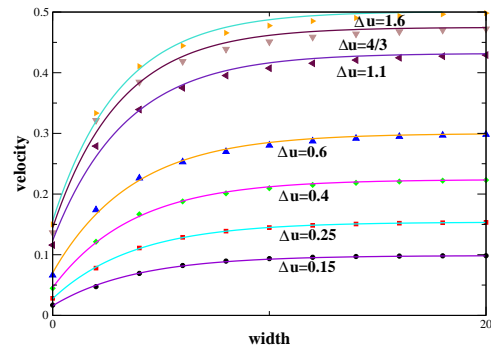


FIG. 5: Plot of $c(w_h)$ as a function of the width w_h of Eq. (4) for different values of Δu as noted against the curves. Solid lines are fits to $c(w) = c_0[1 - a \exp(-w/w_0)]$.

w_h and magnitude of the drive Δu . A small time step is chosen for proper convergence but no spatial continuum limit has been done. We start with a sharp interface, $\phi = 1$ for $0 \leq z \leq L/2$ and $\phi = 0$ for $z > L/2$. A sequential update is done. At every time step, we allow a square pulse of width w_h and strength Δu at the current location of the domain wall or front (located by $\phi = 0.5$). In all cases we observed a monotonic front. Fig. 4 shows the time evolution of the front for the case of a drive with $\Delta u = 0.2$ and of zero width, $w_h = 0$ (pulse at one point of the lattice only).

The variation of the speed with the width of the pulse is shown in Fig 5. Consistent with our results from the variational analysis, we see that the velocity approaches the bulk limit for large widths and this approach is exponential. There is a small but systematic deviation of the observed velocity from the exponential fit for larger values of Δu (in the “unstable” region). Detailed analysis of the pushed versus pulled cases will be reported elsewhere.

In terms of helicases, it seems natural to associate dnaB type passive helicases with the metastable case where the motor action provides the drive that locally disturbs the Y-fork region. As in Ref. [7], we identify the domain wall or the front as the Y-fork region - the junction of the ds-ss DNA. In the metastable case, the pushed dynamics has a stability against small fluctuations, the speed of propagation is independent of the initial conditions, and the speed approaches the steady state limit exponentially in time. All of these are important properties expected of a helicase of type dnaB which after loading on DNA carries out the unzipping in tandem with the other processes during replication.

So far as PcrA (Fig. 1) is concerned, we associate the overall dynamics to the unstable case. No quantitative experimental results are available regarding the magnitude and width of the force PcrA exerts on the bases beyond the Y-fork. It is reasonable to assume that the force is meant to unzip DNA locally, and the effect of this pulling is to make the ds-region unstable. We then infer

that PcrA operates in the unstable ($h > 1/3$) regime. In several mutants of PcrA (replacing a few residues by alanines) the helicase activity (the hand in Fig 1) could be decoupled (reduced) from the motor action and ATP intake (both remained more or less the same). In our terminology, these mutations involve a reduction in h (i.e. the overall pulling strength, Δu , or the width of the pulse, w_h , or both), producing a reduction in the speed as shown in Fig. 5. We like to add that reversed motion of recG can also be understood in the same scheme with a few extra ingredients. This will be discussed elsewhere. Active helicases like PcrA that are involved in repair processes become operational when the replication process stalls because of, e.g., defects. Such a stalling would lead to a relaxation of the stalled front. The new relaxed $\phi(z)$ would then act as the initial condition for the new helicase recruited for repair. The sensitivity to initial condition of a front invading an unstable phase is an important distinction between the metastable (pushed) and the unstable cases. Whether helicases in charge of repair are really sensitive to and recognize these initial conditions need to be tested experimentally.

To summarize, we have proposed a simple coarse grained model for describing helicase activity on DNA. The DNA is described by a local probability of zipping of the base pairs. The motor action of the helicase induces an instability around the front (Y-fork) in an otherwise coexisting zipped and unzipped phases. Such coexisting phases with an interface can in principle be created by pulling or by a stalled helicase on a dsDNA and therefore can be studied experimentally. We have shown that the local drive created by the helicase leads to a traveling front solution with a selected velocity that depends on the nature of the drive. Quantitative studies of forces and sensitivity to the initial conditions would provide crucial clues on the nature of dynamics studied in this paper. We hope single molecular experiments in future would be able to probe these in detail.

-
- * Electronic address: email: somen@iopb.res.in
- [1] B. Alberts *et al*, *Molecular Biology of the Cell*, Garland Pub; 4th edition (March 2002)
 - [2] P.H. von Hippel and E. Delagnotte, *Cell*, **104**, 177-190 (2001); T.M. Lohman and K. P. Bjornson, *Annu. Rev. Biochem.* **65**, 169-214 (1996).
 - [3] S. S. Patel and K. M. Picha, *Ann. Rev. Biochem.* **69**, 651 (2000); D. Fass, C. E. Bogden, J. M. Berger, *Structure* **7** 691 (1999).
 - [4] S. S. Velankar *et al*, *Cell* **97**, 75 (1999); P. Soutanasetal, *EMBO* **19**, 3799 (2000).
 - [5] T. M. Lohman, *J. Bio. Chem.* **268**, 2269 (1993).
 - [6] M. R. Singleton *et al*, *Cell* **107**, 79 (2001).
 - [7] S. M. Bhattacharjee and F. Seno, *J. Phys.* **A 36**, L181 (2003)
 - [8] M. D. Betterton, F. Julicher, physics/0212045
 - [9] Y. Z. Chen *etal* *Phys. Rev.* **E 56**, 919 (1997).
 - [10] S. M. Bhattacharjee, *J. Phys. A* **33**, L423(2000) (cond-mat/9912297);
 - [11] D. Marenduzzo, S.M. Bhattacharjee, A. Maritan, E. Orlandini and F. Seno, *Phys. Rev. Lett.* **88**, 028102 (2002).
 - [12] D. Marenduzzo, A. Trovato and A. Maritan, *Phys. Rev. E* **64**, 031901 (2001).
 - [13] K. L. Sebastian, *Phys. Rev.* **E62**, 1128 (2000).
 - [14] Y. Kafri, D. Mukamel and L. Peliti, *Euro. Phys. J B* **27**, 135 (2002).
 - [15] D. Lubensky and D. R. Nelson, *Phys. Rev. Lett.* **85**, 1572 (2000).
 - [16] S. M. Bhattacharjee and D. Marenduzzo, *J. Phys.* **A 35**, L141 (2002).
 - [17] U. Ebert and W. van Saarloos, *Physica D* **146**,1 (2000). G. Tripathy and W. van Saarloos, *Phys. Rev. Lett.* **85**, 3556 (2000).
 - [18] P.R. Bianco *etal*, *Nature* **409**, 374(2001).; K.M. Dohoney and J. Gelles, *Nature* **409**, 370 (2001).
 - [19] R. D. Benguria and M. C. Depassier, *Phys. Rev. Let.* **77**, 1171(1996).